Detection of Tracker Failures for a 2-Axis Photovoltaic System

Lucas E. A. Barboza[1], Olga de Castro Vilela[1], Gustavo de Novaes Pires[2], Emerson Torres Aguiar Gomes[1], Diego Rodrigues de Miranda[1], João V. F. F. de Medeiros[1] and Leonardo José de Petribú Brennand[1]

[1] Center of Renewable Energy, Federal University of Pernambuco, Recife (Brazil)

[2] Federal Institute of Pernambuco, Recife (Brazil)

Abstract

Solar trackers have been widely used in photovoltaic plants due to the increase in their capacity factor. However, the operation of tracker systems still has challenges, mainly related to failures during operation. The mechanical failures on trackers significantly impact the PV generation and, consequently, have a non-negligible impact on the economic return. The data on trackers' failures in operation situations is rare. The present paper will use a statistical method for daily failure detection from the relation between PV power output and plane-of-array (POA) irradiances. This methodology extracts features from data curves and classifies the days according to them. The accuracy obtained showed that new methods, such as those presented in this paper, may perform better in identifying tracking system failures.

Keywords: sun trackers, anomalies, detection, features, plane-of-array, fault, output power, irradiance

1. Introduction

Solar trackers have been widely used in photovoltaic (PV) plants due to the increase in their capacity factor. Despite this, the presence of trackers introduces uncertainties in the PV plant's performance because the tracking system is a piece of moving equipment. Then, the mechanical failures on trackers have a significant impact on the PV generation and, consequently, a non-negligible impact on the economic return of the plant. Therefore, studying trackers' failures during the operation is crucial. Nevertheless, the data on trackers' failures in operation situations is rare, and the literature on this subject use accelerated tests or others laboratories procedures to understand the phenomenon (Elerath, 2011; Elerath et al., 2011). In this sense, this study aims to develop a methodology for detecting days that the tracking system is stuck in a fixed position in a PV plant, in other words, days that it is not tracking the sun. Based on the Ruth and Muller (2018) publication, the present paper will use a statistical method for failure detection from the relation between the daily time series of the PV output power and plane-of-array (POA) irradiances for a given day.

2. Methods and Materials

Bazovsky (2004) defines failures as an intended period when a device or system does not adequately perform its purpose under operating conditions. From this definition, the main objective of a solar tracker is to increase power production by tracking the sun throughout the day. Thus, even if the tracking system can get stuck all day, if this does not significatively affect the energy production (as is best seen in subsection 3.3), it cannot be considered a failure. Thus, the criterion for determining failures in a tracker is the energy production associated with the photovoltaic system. Moreover, concerning the length of the time considered, it is intuitive to realize that slight deviations in the sun's tracking throughout the day do not generate significant losses in power production. In this sense, it is appropriate to consider the day as the scale of the time considered for the failure analysis. Therefore, this work will focus on daily failures.

The main idea of daily tacker failure detection is based on the relation between the time series of PV output power

Selection and/or peer review under responsibility of Scientific Committee
doi:10.18086/eurosun.2022.16.02 Available at http://proceedings.ises.org

and plane-of-array (POA) irradiance (Ruth and Muller, 2018). As shown in Fig. 1, when the tracker functions as expected, the power curve has a shape similar to the POA curve for a system tracking the sun. On the other hand, when the tracker is stuck, the power curve is similar to the POA curve for a fixed collector (Fig. 2).

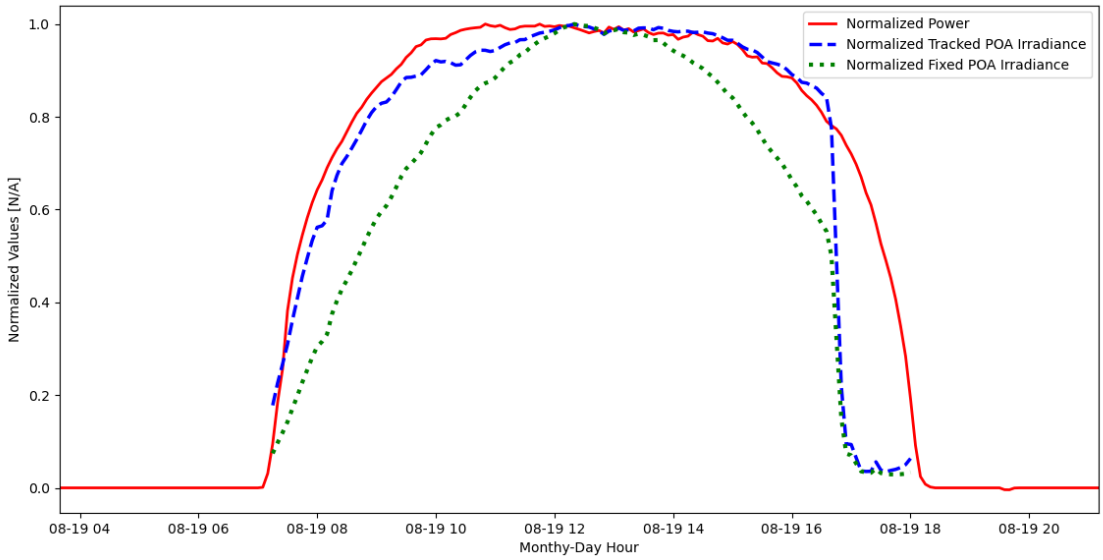

Fig. 1: Daily time series of PV output power and POA irradiances for a solar PV system with a dual-axis tracker, at site 2 in Desert Knowledge Australia Solar Centre, in Alice Springs, Central Australia, on August 19th, 2012. The solid red line represents the measured power; the dashed blue line is the dual-axis POA; the green dotted line the fixed-tilt POA. Note that when the tracker is working, the power curve is similar to the POA curve for a tracking collector.

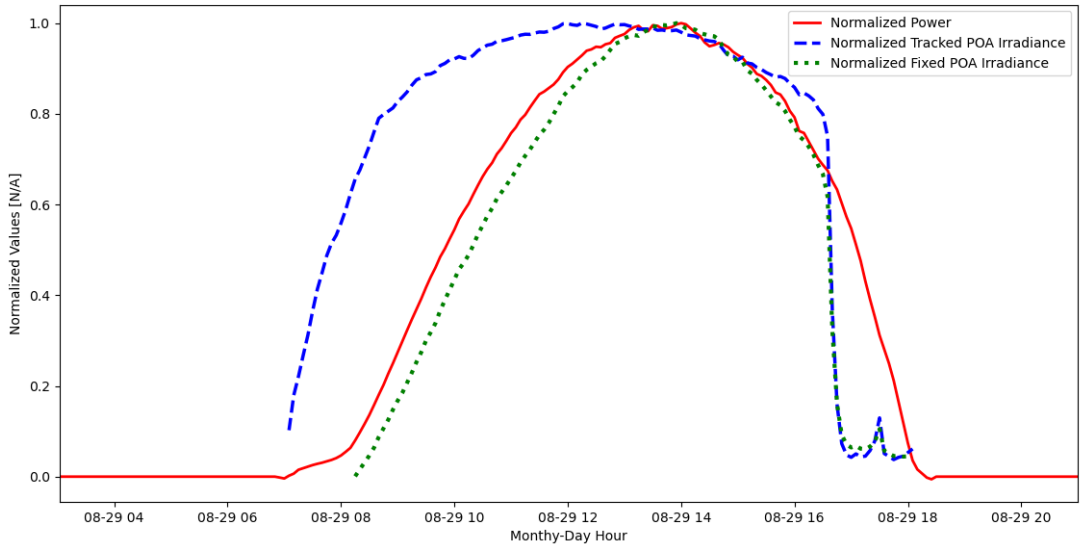

Fig. 2: Daily time series of PV output power and POA irradiances for a solar PV system with a dual-axis tracker, at site 2 in Desert Knowledge Australia Solar Centre, in Alice Springs, Central Australia, on August 29th, 2012. The solid red line represents the measured power; the dashed blue line is the dual-axis POA; the green dotted line the fixed-tilt POA. Note that when the tracker was stuck, the power curve was similar to the POA curve for a fixed collector.

3.1. Methodology

Plane-of-array (POA) irradiance is the total irradiance arriving at the collector plane (a tilted PV panel, for instance). This collector can be in a fixed position or moving from a tracking system. Usually, we obtain POA irradiance from local measurements of global (G), beam (G_b), and diffuse (G_d) irradiances in the horizontal plane. Eq. 1 shows the relation between G, G_b, and G_d, involving the azimuth angle θ_Z. If one of these horizontal irradiances isn't available, we can determine the missing irradiance from the other two. The eq. 2 shows how to calculate POA from G, G_b, and G_d, where β is the collector tilt angle, and 0.2 is the albedo (fraction of irradiance reflected by the ground). The angle θ is the incidence angle between the sun rays and the collector normal line. θ has a different expression for collectors fixed installed and for collectors with solar trackers. Tab. 1 presents the incidence and collector tilt angles for fixed and dual-axis systems (Rabl, 1985). It is necessary local latitude Φ, declination δ, and hour ω angles of the sun, azimuth γ and inclination β angles of the collector for eq.2. The expressions of these angles and their references can be found in Rabl (1985).

$$G = G_b \cos\theta_Z + G_d \qquad \text{(eq. 1)}$$

$$POA = G_b \times \cos\theta + {}^1\!/_2 \times G_d \times (1 + \cos\beta) + {}^1\!/_2 \times 0.2 \times G(1 - \cos\beta) \qquad \text{(eq. 2)}$$

Tab. 1: Cosine of incidence angle value for a tilted fixed collector, and a collector with dual axis tracker

	Tilted Fixed Collector	**Collector with dual axis tracker**
Cosine of incidence angle θ	$\cos\delta\cos\Phi\cos\beta\cos\omega + \sin\delta\sin\Phi\cos\beta + \cos\delta\sin\gamma\sin\beta\sin\omega + \cos\delta\cos\gamma\sin\Phi\sin\beta\cos\omega - \sin\delta\cos\Phi\sin\beta\cos\gamma$	1
Collector tilt angle β	Collector fixed tilt angle	Zenith angle θ_Z

Source: Rabl (1985).

In this context, the present methodology extracts three features from POA and output power curves aiming to identify daily tracker failures. First of all, the curves are normalized by their maximum values of the day. This normalization allows comparing two variables with different units: irradiance and power. The first feature is the Pearson correlation between the output power and the tracked collector POA irradiance, which reveals if the tracker is working as expected for a given day. The next step is comparing the output power with a fixed collector POA irradiance. For this comparison, the methodology sets a range of possible tracker stuck positions, calculates the Pearson correlation between the correspondent POA irradiance and power curves, and chooses the position with the most significant value. This procedure is necessary because there is no information about the precise stuck position. The third feature is also related to a fault in the tracking system. It involves the error curve, i.e., the curve resulting from the element-wise difference between the normalized series of output power and tracked POA irradiance. The error curve has a characteristic shape for stuck tracker days, as shown in Fig. 3. So, the feature extracted is the Pearson correlation between the real error curve (using real output power time series) and the theoretical error curve. This theoretical curve uses the modelled power instead of the actual power output. In this step, the stuck position is found for the second feature and is used to calculate the theoretical power from eq. 3 (Abd El-Aal et al., 2006; Navarte and Lorenzo, 2008). The nominal generator power P_{NOM}, the efficiency η, the power temperature loss coefficient β, and the coefficient K are constants in eq.3; and ambient temperature T_{AMB}, and POA irradiance are inputs of the model. The PV module datasheet informs the β value, and 0.03 is a good

approximation for K (Fuentes et al., 2007). The trust region reflective non-linear least squares method calculates the coefficient value η that best fits the data (Li, 1993).

$$P = \eta\, P_{NOM} \frac{POA}{1000}\{1 - \beta[(T_A + K \times POA) - 25]\} \qquad \text{(eq. 3)}$$

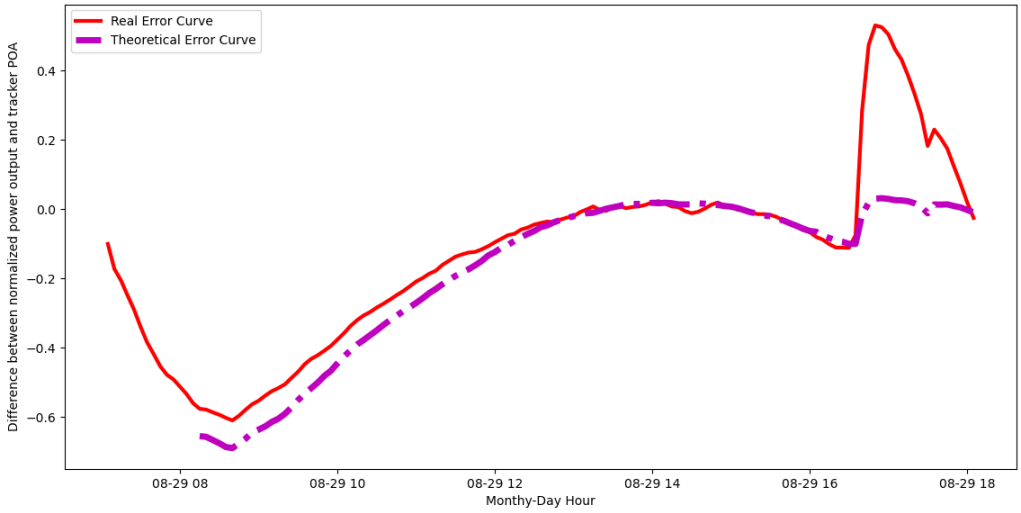

Fig. 3: Error Curves for a solar PV system with a dual-axis tracker failure at site 2 in Desert Knowledge Australia Solar Centre, in Alice Springs, Central Australia, on August 29th, 2012. These curves result from the element-wise difference between normalized series of power and normalized tracked POA. The solid red line represents the error curve obtained using the actual power output; the dashed magenta line is obtained using modelled output power.

The features used in the model are functioning correlation, fixed correlation, and error curve correlation. So, the method selects the days from the dataset and calculates these three features for each day. An interval value must be determined for a feature to classify a day as tracker functioning or tracker stuck. Since all features are Pearson correlations, we assume an interval that ends at one and begins at one minus 15% of the standard deviation of the corresponding feature series. So, the classification of days inside these ranges are tracker functioning, or tracker stuck: in the functioning correlation method, set as functioned; in the fixed or error curve correlations methods, selected as failed.

3.2. Observational Data

The sample data analysed in this work is from a 26.5kW photovoltaic system (Fig. 4) at the Desert Knowledge Australia Solar Centre (DKASC-2), site 2 in Alice Springs, Central Australia, at a longitude of 133.87°W and latitude of 23.76°S (DKA, n.d.). Between August 24th, 2010 to December 1st, 2012, a dual-axis tracker was working at the site. The lifetime of the tracking device totals 830 days. In addition, there are also some records of the maintenance staff during this period. The DKASC-2 data contain G, G_d and active power output, with a timestep of 5 minutes. The coefficients η, β and K from eq. 3 for DKASC-2 are in Tab. 2.

Tab. 2: The coefficients η, β and K from eq. 3 for DKASC-2.

η	β	K
0.75	$0.0045\ °C^{-1}$	$0.03\ °C\ W^{-1}m^2$

Fig. 4: The dual-axis tracker 26.5kW photovoltaic system of site 2 of the Desert Knowledge Australia Solar Centre (DKASC-2), in Alice Springs, Central Australia, working between August 24th,2010 to December 1st, 2012. Source: DKA.

3.3. Visual Inspection

The 830 days of the dual-axis tracker lifetime have visually been analyzed to identify failures aiming to validate the methodology explained in subsection 3.2. The days have been classified into function, failures, undetermined and missing. Curves like the left in Fig.1 are classified as 'function'; curves like the right in Fig.1 as 'failure'. The days when the maintenance staff identifies periods in which the tracker is stuck are set as failure days too. For instance, the tracker was stuck in a fixed position from March 22th, 2012, to May 30th, 2012, due to a porous clamp housing (DKA, n.d.). 'Missing' are days when power or irradiances daily series have less than half the expected sample data. Finally, as shown in Fig. 5, 'undetermined' are days when it is impossible to know whether the tracker is working. On the undetermined days, whether the tracker is working does not affect the daily power generation because many other problems could occur; then, it cannot be classified as 'failure'. On the other hand, it is impossible to ensure that the tracking system functioned as expected. In other words, in the absence of maintenance notes, on undetermined days (usually cloudy days), the tracker is in a simultaneous functionally and failure state due to visual inspection method limitation, and, it is not possible to ensure 'function' or 'failure' class to that day.

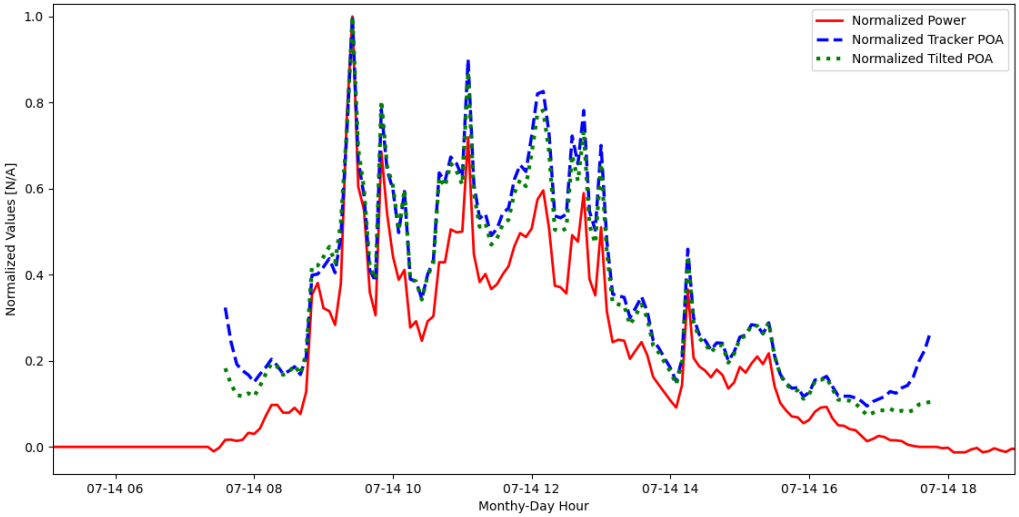

Fig. 5: Daily time series of PV output power and POA irradiances for DKASC-2 on July 12th, 2011. The solid red line represents the measured power; the dashed blue line is the dual-axis POA; the green dotted line the fixed-tilt POA. These days are classified as undetermined because visual inspection cannot determine the failure.

3.4. Model Performance Metrics

In the model performance analysis, the undetermined and missing days will be excluded from the control dataset because they do not assure if the tracker is functional or not, as explained in subsection 3.3. The present work uses confusion matrix and accuracy as model performance metrics (Costa et al., 2007). These metrics use the numbers of true and false positives (TP and TF, respectively) and true and false negatives (TN and FN, respectively). In this sense, the positive in the methodology using functioning correlation is identified as functional tracker days, while the method using fixed or error curve correlations is to identify tracker failure days. Tab. 3 shows the principle of a confusion matrix, and eq. 4 presents the formula for accuracy.

Tab. 3: Confusion Matrix.

	Predicted Class	
True Class	Positive	Negative
Positive	True positive (TP)	False negative (FN)
Negative	False positive (FP)	True negative (TN)

$$A_{CC} = \frac{TP+TN}{TP+FP+FN+TN} \qquad \text{(eq. 4)}$$

3. Results and Discussion

Tab. 4 shows the accuracies for each method. Remember that the missing and undetermined days are excluded from the control dataset for the accuracy calculation. The error curve correlation presents the best result in predicting the target, followed by fixed correlation and functioning correlation. In this sense, the methods that directly use the correlation between power and POA curves have the worst performances, while the process that uses an intermediate step (the error curve) has the best accuracy. This procedure differs from what Ruth and Muller (2018) found in their work. In Ruth and Muller's work, they used functioning and fixed correlations and achieved good results. Perhaps, this difference is because the present work uses sample data of a dual-axis tracker, not a single-axis. Then, the result suggests that using other features and methods can increase the models' performance.

Tab. 4: Confusion Matrix for DKASC-2 Error Curve Correlation series. Undetermined and missing days have been excluded from the control dataset.

Method	Accuracy
Functioning Correlation	0.49
Fixed Correlation	0.80
Error Curve Correlation	0.90

Fig. 6, Fig. 7 and Fig. 8 show the functional, fixed, and error curve correlations series, the classification obtained by visual inspection in each one, and their respective classification thresholds. Note that there is a kind of information complementarity, i.e., when a day is not set as a 'failure' day in the methods of error curve or fixed, it is because it is supposed to be classified as a 'function' day. Tab. 5, Tab. 6 and Tab. 7 present the confusion matrices.

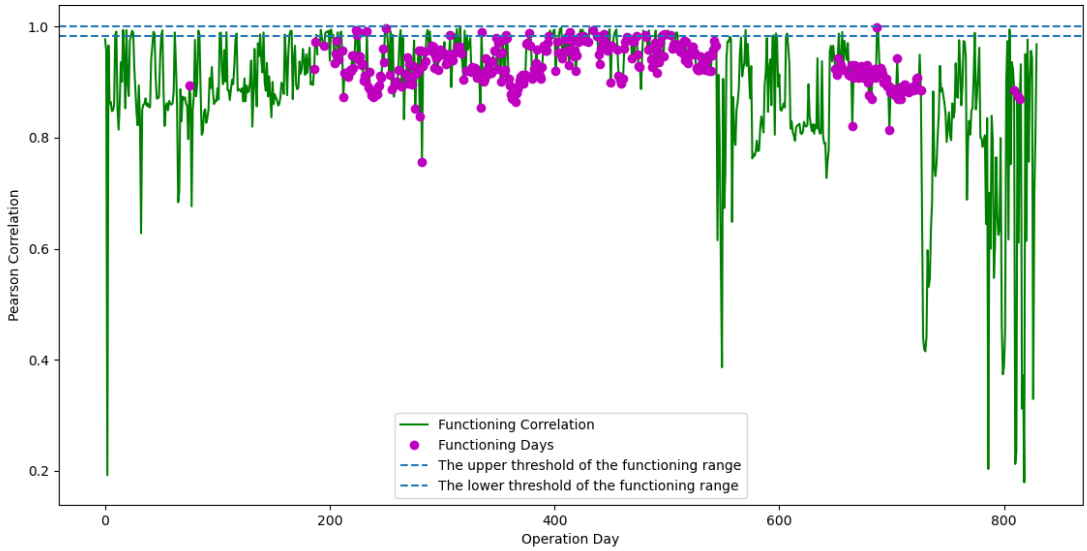

Fig. 6: Functional Correlation series for DKASC-2. The solid green line represents the correlation values; the magenta dots are the functional days identified in the visual inspection; the blue dashed lines represent the lower and upper range limits of detection of functioning days.

Tab. 5: Confusion Matrix for DKASC-2 Functional Correlation series. Undetermined and missing days have been excluded from the control dataset.

	Predicted Class	
True Class	Positive	Negative
Positive	17	324
Negative	0	294

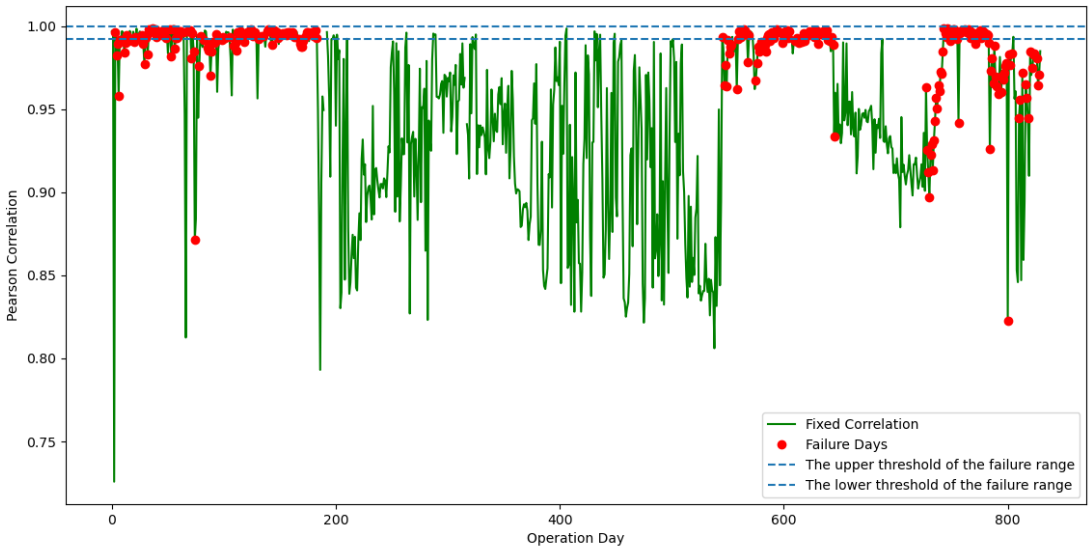

Fig. 7: Fixed Correlation series for DKASC-2. The solid green line represents the correlation values; the red dots are the failure days identified in the visual inspection; the blue dashed lines represent the lower and upper range limits of detection of failure days.

Tab. 6: Confusion Matrix for DKASC-2 Fixed Correlation series. Undetermined and missing days have been excluded from the control dataset.

	Predicted Class	
True Class	Positive	Negative
Positive	167	127
Negative	0	341

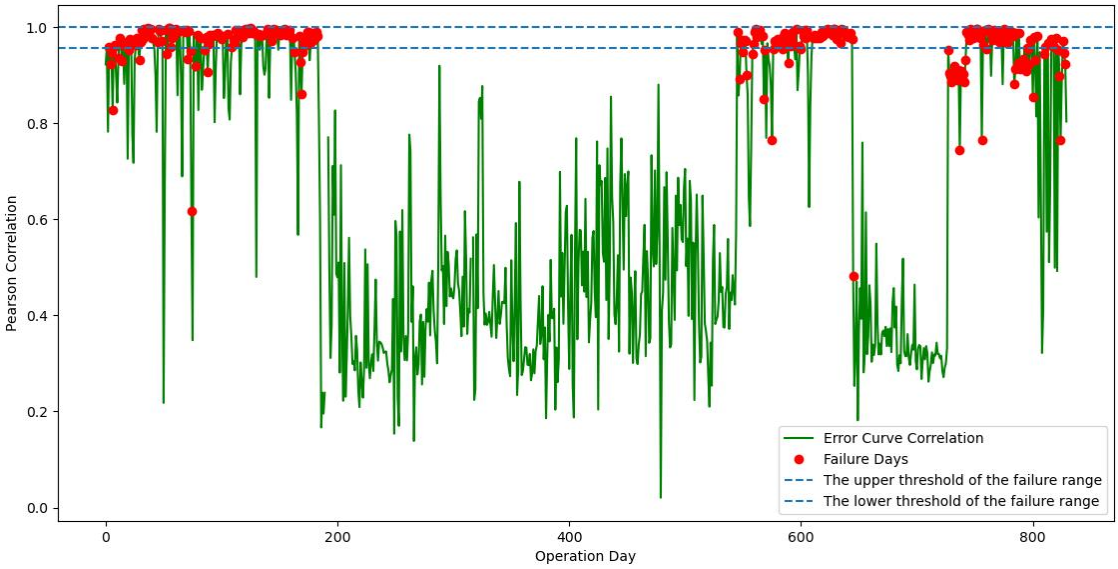

Fig. 8: Error Curve Correlation series for DKASC-2. The solid green line represents the correlation values; the red dots are the failure days identified in the visual inspection; the blue dashed lines represent the lower and upper range limits of detection of failure days.

Tab. 7: Confusion Matrix for DKASC-2 Error Curve Correlation series. Undetermined and missing days have been excluded from the control dataset.

	Predicted Class	
True Class	Positive	Negative
Positive	228	66
Negative	0	341

4. Conclusions

The work extracts features for each day of data from DKASC-2. The objective was to identify daily failures and regular working days by three features: functioning correlation, fixed correlation and error curve correlation. Different from Ruth and Muller (2018) paper, the results show that the error curve had the best accuracy, which indicates that developing more methods could increase detection performance. Furthermore, the three methods have a kind of complementarity of information that needs further studies.

5. Acknowledgments

The authors are grateful to the Desert Knowledge Australia Centre (e.g. Alice Springs) for the data provided, to the Brazilian Higher Education Personnel Improvement Coordination - CAPES and to the Postgraduate Program in Energy and Nuclear Technologies - PROTEN of Federal University of Pernambuco, Brazil. Finally, we also thank the Center of Renewable Energy (CER) team at the Federal University of Pernambuco.

6. References

Abd El-Aal, A. E. M. M., Schmid, J., Bard, J., & Caselitz, P. (2006). Modeling and optimizing the size of the

power conditioning unit for photovoltaic systems. Journal of Solar Energy Engineering, 128(1), 40-44.

Bazovsky, Igor. Reliability theory and practice. Courier Corporation, 2004.

Costa, E., Lorena, A., Carvalho, A. C. P. L. F., Freitas, A. 2007, July. A review of performance evaluation measures for hierarchical classifiers. In Evaluation methods for machine learning II: Papers from the AAAI-2007 workshop. pp. 1-6.

DKA, n.d. Desert Knowledge Australia Centre. Download Data. [WWW Document]. URL http://dkasolarcentre.com.au/download?location=alice-springs (accessed 11.16.21).

Elerath, J.G., 2011. Reliability assessment of high-concentration photovoltaic trackers, in: Proceedings - Annual Reliability and Maintainability Symposium. pp. 1–6. https://doi.org/10.1109/RAMS.2011.5754525

Elerath, J.G., Spencer, M., Horne, S., 2011. Demonstrating reliability in HCPV systems, in: 37th IEEE Photovoltaic Specialists Conference. IEEE, pp. 3547–3552. https://doi.org/10.1109/PVSC.2011.6185910

Fuentes, M., Nofuentes, G., Aguilera, J., Talavera, D. L., & Castro, M. (2007). Application and validation of algebraic methods to predict the behaviour of crystalline silicon PV modules in Mediterranean climates. Solar Energy, 81(11), 1396-1408.

Li, Yuying. 1993. Centering, trust region, reflective techniques for nonlinear minimization subject to bounds. Cornell University. https://hdl.handle.net/1813/6159

Narvarte, L., Lorenzo, E. (2008). Tracking and ground cover ratio. Progress in photovoltaics: research and applications, 16(8), 703-714.

Rabl, A., Oxford, N.Y., 1985. Active Solar Collectors and Their Applications, 1st ed. Oxford University Press, Inc, New York.

Ruth, D., Muller, M., 2018. A methodology to analyze photovoltaic tracker uptime. Progress in Photovoltaics: Research and Applications 26, 491–501. https://doi.org/10.1002/pip.3002